



PLAXIS

Rock reinforcement modelling

PLAXIS 2D CONNECT EDITION V22.02

Table of Contents

1	Introduction.....	1
2	Example case definition	2
2.1	Model geometry	2
2.2	Material properties	3
3	Numerical analysis	5
3.1	Modelling of construction phases	5
3.2	Analysis of results	7
4	Conclusions	8
5	References	8

1

Introduction

Rock reinforcements have been widely used in rock engineering practice and represent a dominant system in mines and underground structures. Even though the term support is generically used to describe the procedures and materials used to improve the stability and maintain the load-carrying capability of rock near the boundaries of underground excavations, a distinction is made between the terms reinforcement and support. In accordance with modern practice (Windsor and Thompson, 1993), support is the application of a reactive force to the surface of excavation and includes techniques and devices such as timber, fill, shotcrete, mesh and steel or concrete sets or liners; while reinforcement is a means of conserving or improving the overall rock mass properties from within the rock mass by techniques such as rock bolts, cable bolts and ground anchors.

A reinforcement system is comprised of components that dictate with their interaction the mechanical behaviour and the performance of all types of reinforcements:

Based on their coupling mechanism, rock reinforcements can be classified as (Windsor, 1997):

1. Discretely Mechanically or Frictionally Coupled (DMFC): these systems are anchored in the borehole at one or more discrete points and the main types belonging to this category are two-point anchored bolts (i.e., expansion shell bolts and bolts anchored by a slit and wedge mechanism) and end grouted anchor bolts;
2. Continuously Frictionally Coupled (CFC): these systems are bound to the rock mass mainly via frictional resistance along their entire length and are thus commonly referred to as frictional bolts (i.e., split set and inflatable bolts); and
3. Continuously Mechanically Coupled (CMC): these systems are characterized by an internal solid bar (i.e., fully-grouted rebar) or stranded wire cable bound to the rock through a cementitious or resin-based grout.

Rock reinforcements can also be distinguished in active (e.g., strand cable) and passive (frictional bolts) systems depending on whether they can or cannot be tensioned at the time of the installation. Passive/untensioned reinforcements are often called dowels.

Rock reinforcement systems in PLAXIS have been classically modelled by relying on available structural elements such as node-to-node anchor (e.g., two-point anchored bolt), embedded beam (e.g., frictional or grouted bolts) or a combination of these two elements (e.g., end-grouted anchor bolt). In addition, for those systems involving the usage of node-to-node anchor, the pre-tensioning during the installation phases can also be simulated (e.g., active DMFC systems).

Recently, a new element, namely “Cable bolt”, has been introduced in PLAXIS, which can be used to model all the mentioned systems (including DMFC reinforcements) as long as bending is negligible, and also to simulate the pre-tensioning for all active systems (including CMC reinforcements). Moreover, this versatile element allows for a more straightforward definition of the reinforcement parameters as well as their calibration against specific test results for the evaluation of mechanical parameters (i.e., pull-out tests). In order to show the usage of the new cable bolt elements within the PLAXIS workflow along with the definition of the parameters for this type of reinforcement system, this document provides a practical example of an underground excavation reinforced with cable elements.

Example case definition

The practical example concerns a reinforced mine drift with typical geometrical characteristics and reinforcement systems of underground mining operations, suitable for the encountered in-situ stress conditions and rock mass properties.

2.1 Model geometry

A horseshoe-shaped drift 4.8 m wide and 4.8 m high within a homogeneous rock mass is considered in this example case.

The drift is located 350 m below the surface and subjected to an in-situ stress of 10 MPa. To avoid the modelling of the entire overburden rock mass and reduce the model size, the *Field stress* option is adopted to define the magnitude and orientation of the in-situ stress conditions. To prevent that the boundaries of the model influence the results, the domain is extended to more than ten times the size of the cavity: the model dimensions are set to 60 m wide and 60 m high.

The drift excavation is reinforced with a set of cable bolts with length of 2.4 m and spaced along the boundary of the excavation of 1.2 m, for a total of 9 installed elements.

Figure 2.1 shows the model geometry along with the finite element mesh used in this example. It should be noted that the model also shows another horseshoe-shaped geometry around the reinforced excavation with the aim of controlling the mesh finesses in that area. This is necessary since, if only the mesh in the tunnel was refined, a too rapid transition to larger elements would occur, affecting the accuracy of the solution in the zone of interest.

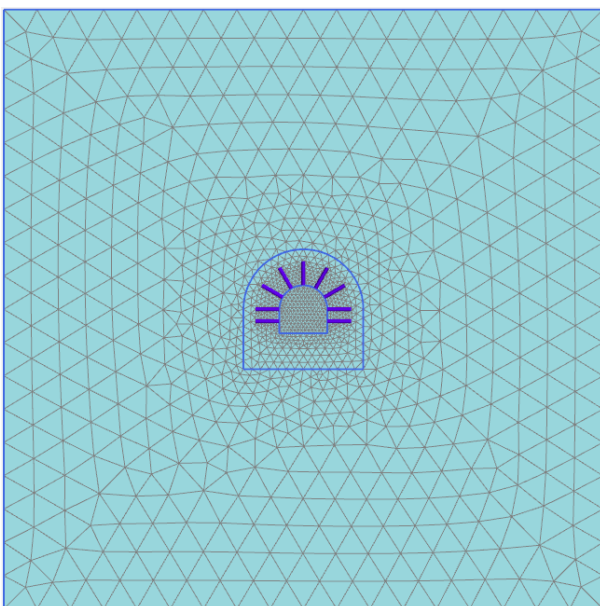


Figure 2.1: Geometry of the tunnel

2.2 Material properties

The drift is excavated in a fair-quality rock mass characterized by a GSI value of 50 and modelled using the Hoek-Brown model. The parameters characterizing the mechanical behaviour of the rock mass are summarized in Table 2.1.

Table 2.1: Rock mass properties

PARAMETER	SYMBOL	LINING	UNITS
Young's modulus	E_{rm}	10	GPa
Poisson's ratio	ν	0.25	-
Intact rock compressive strength	σ_{ci}	30	MPa
Intact rock Hoek-Brown parameter	m_i	10	-
Geological Strength Index	GSI	50	-
Disturbance factor	D	0	-
Max dilation angle (ψ at $\sigma_3 = 0$)	ψ_{max}	20	°
Confining pressure (σ_3 at $\psi = 0$)	σ_{ψ}	100	MPa

The reinforcement system is made of 25.4 mm-diameter grouted cable elements, installed at 1.2 m spacing perpendicularly to the analysis plane and characterized by the properties reported in Table 2.2.

Table 2.2: Cable bolt properties

PARAMETER	SYMBOL	LINING	UNITS
Out-of-plane spacing	$L_{spacing}$	1.2	m
Diameter	D	25.4	mm
Axial stiffness	E	98.6	GPa
Tension limit	$N_{p,tens}$	548	kN
Shear stiffness	k_s	15	GN/m ²
Bond cohesive strength	c_{bond}	800	kN/m
Bond frictional angle	φ_{bond}	20	°

The axial stiffness E and tension limit $N_{p,tens}$ control the axial behaviour of the reinforcing element. The shear stiffness, the cohesive strength and friction angle are the bond properties (Figure 2.2) controlling the shear behaviour of the grout annulus. In particular, the last two parameters provide the bond strength capacity (maximum shear strength) of the grout as a function of its cohesive strength and stress-dependent frictional resistance through the following relation:

$$T_{s,bond,max} = c_{bond} + \sigma_n \tan(\varphi_{bond}) \cdot Perimeter \quad Eq. 2.1$$

where σ_n is the confining stress normal to the cable axis while *Perimeter* refers to the exposed failure perimeter of the element (assuming that failure can occur either at the cable/grout or the grout/rock

interface). It should be noted that the confining stress is calculated based on the current stress state in the rock mass surrounding the cable bolt.

As far as the *Failure surface perimeter* option is concerned in this example, the *Predefined* option has been adopted (Figure 2.2), which assumes that *Perimeter* is calculated based on the cable diameter, meaning that failure takes place at the cable/grout interface.

General		Mechanical	
Property	Unit	Value	
Properties			
L_{spacing}	m	1.200	
Cross section type		Predefined	▼
Predefined cross section type		Solid circular beam	▼
Diameter	m	0.02540	
A	m ²	0.5067E-3	
Stiffness			
E	kN/m ²	98.60E6	
Strength			
$N_{p,\text{comp}}$	kN	0.000	
$N_{p,\text{tens}}$	kN	548.0	
Bond stiffness			
Shear stiffness k_s	kN/m ²	15.00E6	
Bond strength			
Fully bonded		<input type="checkbox"/>	
Strength distribution		Uniform	▼
Cohesive strength	kN/m	800.0	
Φ_{bond}	°	20.00	
Failure surface perimeter		Predefined	▼
Perimeter	m	0.07980	

Figure 2.2: Cable bolt material properties

The bond stiffness and strength can usually be measured directly through pull-out tests. Alternatively, they can be reasonably estimated through empirical relationships proposed by St. John and Van Dillen (1983) as a function of the compressive grout strength, shear modulus and annular thickness.

3

Numerical analysis

3.1 Modelling of construction phases

The mine drift excavation modelling has to simulate the advancement of the face of the drift and the installation of the reinforcement at a certain distance behind the face. This implies that the load redistribution and the corresponding displacements of the unsupported part of the excavation is initially carried out by the face itself. As the drift face advance and reinforcement system is installed this last will contribute to carry the remaining portion of the redistributed load due to the advancement of the excavation. To simulate this 3D “face effect” in PLAXIS 2D, the *Deconfinement* (ranging from 0% to 100%) option can be used: as the *Deconfinement* increases in value the rock mass loses its confinement effect due to the vicinity of the excavation face. As further detailed later in the text, this mine drift example considers that the installation of the cable bolts takes place once 30% of confinement loss has occurred.

The installation of the cable bolts considers that the cables are pre-tensioned with a force equal to 300 kN before the grouting is finalized. The simulation of this installation step is facilitated by the available *Adjust prestress* option. To be able to apply a pre-tension to a cable element, the end part (embedded in the rock mass) should be practically bonded, meaning that the end node should be considered tied to the rock mass.

However, during pre-stressing, this would generate local tensile stresses around that location, requiring then that a proper tensile strength is assigned to the rock mass. A more realistic approach for modelling the pre-tensioning process is that each cable is split into a bonded part and a free (unbonded) part. With this approach, the pre-tensioning force can be transferred to the rock mass via an appropriate bonded length to avoid unrealistic stress localization. The free part will be bonded automatically after deselecting the *Adjust prestress* option.

This latter modelling procedure is adopted in this example where a 0.8 m long bonded part and a 1.6 m long (initially) free part (bond interaction is automatically inactive) are considered in the pre-tensioning phase.

Additionally, the cable bolts are considered *Connected* to the excavation surface (the rock mass) for simulating the external fixture through a face plate.

To simulate the operational procedure described above, the following four calculation phases will be defined in the *Staged Construction* mode:

Initial Phase

In this phase, initial stresses are generated using the *Field stress* procedure, by initializing the model with a compressive stress of -10 MPa for both vertical and horizontal stress components.

For proper use of the *Field stress* option, all boundaries should be fixed. This can be setup via the *Model Conditions>Deformations* in the *Model Explorer*.

First phase excavation

During this phase, the drift is excavated while the cable bolts remain inactive. The to be excavated rock mass is deactivated and a *Deconfinement* of 30% is applied.

Cable bolt installation

This phase deals with the cable bolt installation. Both bonded and free parts are activated and pre-tensioning takes place by selecting the *Adjust prestress* check box in the *Selection explorer*. A value of 300 kN for the prestress force ($F_{prestress}$) is entered in the corresponding edit box, as shown in Figure 3.1. It should be noted that the *State* box in the *Selection explorer* is automatically set to *Unbonded* and *Bonded* for the free and grouted portions, respectively.

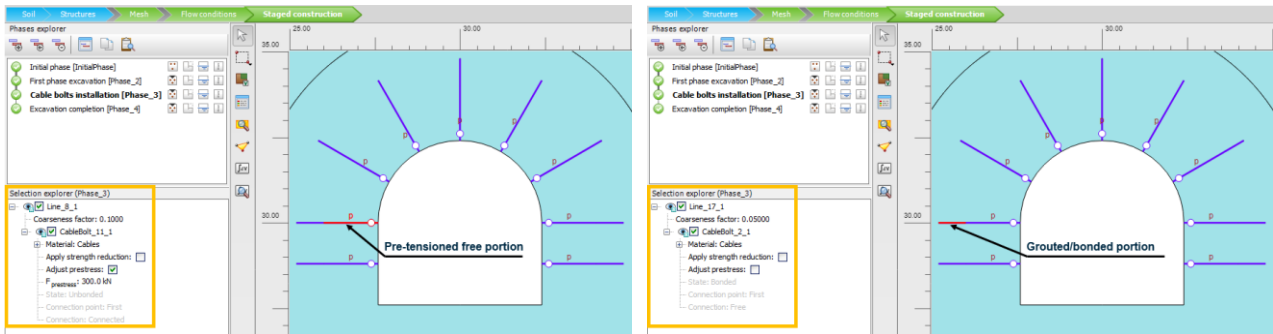


Figure 3.1: Cable bolt installation: pre-tensioned free portion (left) and grouted/bonded portion (right). Geometry of the tunnel

Excavation completion

In this last phase, the *Adjust prestress* check box is deselected, allowing bond interaction with the surrounding rock mass to develop also in this portion of the bolt, as shown in Figure 3.2. The *Deconfinement* is set to 100% to account for solving the remaining unbalance of the excavation as well as the unbalance caused by installing the pre-tensioned reinforcement elements.

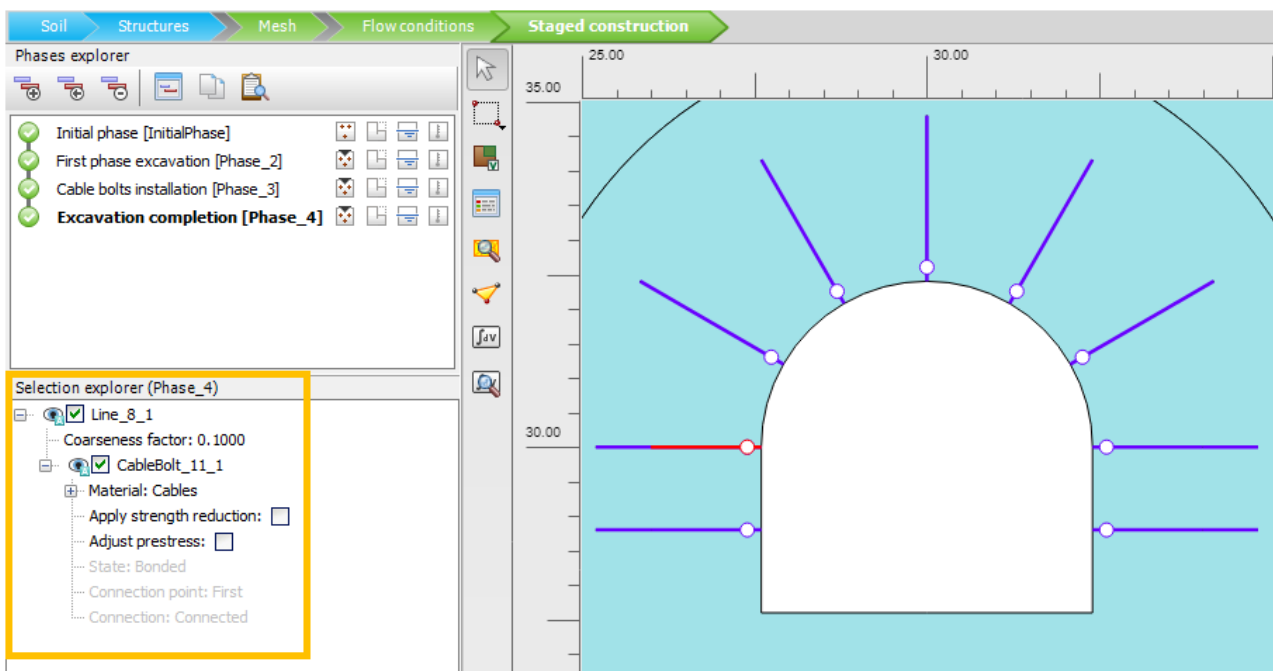


Figure 3.2: Geometry of the tunnel

Once all phases are defined, the calculation can simply be executed using default settings.

3.2 Analysis of results

The cable bolts behaviour is investigated by showing the forces generated along them during the installation and operational phases. Figure 3.3 shows the force and the mobilized shear per cable generated during the pre-tensioning phase. It can be observed that, due to the effect of pre-tensioning, the tensional forces (*Axial forces N*) develop only along the unbonded portion of the cable elements with a value accounting for the out-of-plane spacing of 1.2 m. On the other hand, the bond strength $T_{s,bond}$ is mobilized only along the grouted/bonded portion of the cable elements.

In the subsequent construction phase, when the grouting is completed along the entire length of the cable bolts, the axial forces due to the previously applied pre-tensioning represent only an initial state, meaning that these will now evolve in response to the further progress of the excavation and consequent deformation of the rock mass. Figure 3.4 shows the tensional forces generated in the cable elements once the excavation phase is completed (*Deconfinement* equal to 100%). It should be noted that tensional capacity is almost approached since the maximum generated force (453.5 kN/m, or with a spacing on 1.2 m: $453.5 \text{ kN/m} \times 1.2 \text{ m} = 542.6 \text{ kN/cable bolt}$) is close to the tensional limit (548 kN/cable bolt).

To highlight the role of the stress-dependent (frictional) quota of the bond strength, the maximum shear force in the bond at the current confinement stress ($T_{s,bond,max}$ – the shear force limit for the $T_{s,bond}$) along the cable length is plotted in Figure 3.4. It is evident that the distribution of the bond strength along the cable complies with the variation of the confining stress, which, in turn, depends on the current stress state in the rock mass surrounding the excavation (increasing with the distance from the excavation boundary).

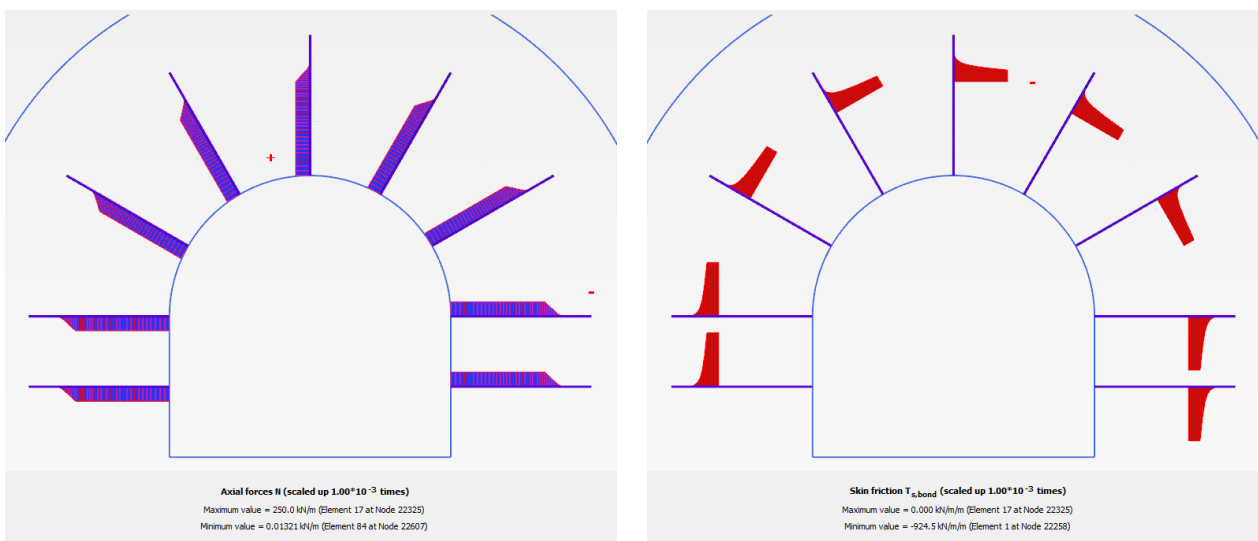


Figure 3.3: Cable bolt installation: pre-tension force on unbonded part (left) and bond strength mobilization on grouted part (right).

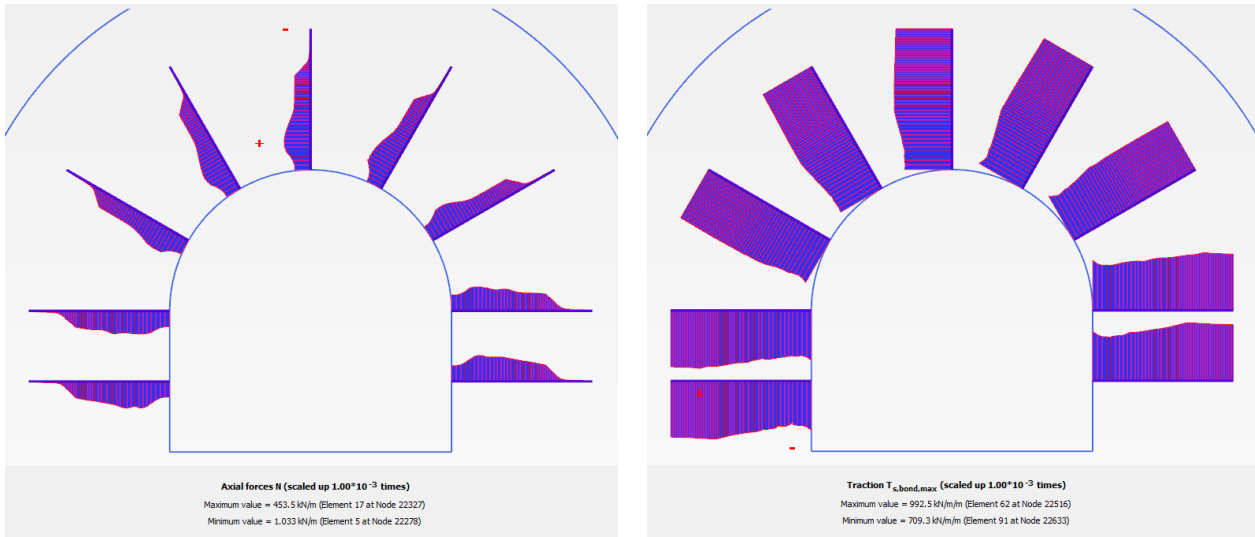


Figure 3.4: Excavation completion: axial forces on grouted cable bolts (left) and bond strength limit (right).

4

Conclusions

In this document, the new cable bolt element available in PLAXIS has been briefly introduced by reporting its main capabilities, i.e., the axial-only behaviour, the prestressing option, and the definition of the bond strength.

The required mechanical parameters along with the operational behaviour of this new structural element, have been demonstrated through an engineering application consisting of a mine drift excavation reinforced with pre-tensioned cable bolts.

It is evident how this new structural element complements existing capabilities of PLAXIS for rock engineering practitioners, allowing them to benefit from robust, efficient, and easily calibratable modelling.

References

St. John, C. M., and D. E. Van Dillen, 1983, *Rockbolts: A New Numerical Representation and Its Application in Tunnel Design*, in *Rock Mechanics – Theory - Experiment – Practice* (Proceedings of the 24th U.S. Symposium on Rock Mechanics, Texas A&M University, June 1983), pp. 13-26. New York: Association of Engineering Geologists

Windsor, C. R. and Thompson, A. G., 1993, *Rock reinforcement – technology, testing, design and evaluation*, *Comprehensive Rock Engineering* (eds J. A. Hudson, E. T. Brown, E. Hoek and C. Fairhurst), 4: 451–84. Pergamon: Oxford.

Windsor, C. R., 1997, *Rock reinforcement systems*, *Int. J. of Rock Mech. Min. Sci.* 34 (6), 919–951